Direct Luminescence Chronology of the Epipaleolithic Kebaran Site of Nahal Hadera V, Israel

D.I. Godfrey-Smith,[1] K.B. Vaughan,[1] A. Gopher,[2] and R. Barkai[2]

[1]*Department of Earth Sciences, Dalhousie University, Halifax, Nova Scotia, B3H 3J5, Canada*
[2]*Department of Archaeology, Tel Aviv University, Ramat Aviv 69978, Israel*

We report direct luminescence ages for the culture-bearing sediments of the Kebaran site of Nahal Hadera V (NHV) in the coastal plain of Israel. Although the site contains, in addition to rich lithic deposits, plentiful mammalian bone, it has proved to be undatable using radiocarbon dating, in spite of the fact that the cultural context places the time of occupation well within the range of radiocarbon dating. In contrast, luminescence dating of the site sediments proved successful. Luminescence ages were determined using the single aliquot additive-dose (SAA) method, applied to sand-sized quartz extracts to determine past equivalent doses (D_e). Dose rates (R) were calculated using thick source alpha counting for the uranium (U) and thorium (Th) concentrations and x-ray fluorescence analysis for the potassium (K_20) concentration. Of the five samples collected at the site, four represent cultural and subcultural deposits and the fifth represents the geological substrate for the archaeological deposit, a quartz-rich, carbonate-cemented dune sand known as aeolianite or kurkar. The luminescence age of the kurkar is 42.7 ± 6.3 ka. Human occupation of the site occurred between 21.3 ka and 14.0 ka ago, during the Last Glacial Maximum.

INTRODUCTION

The Epipaleolithic Period in the Levant spans the time from approximately 22,500–12,500 calibrated years before present (cal yr B.P.) and is considered a bridge between the hunter-gatherer lifestyle of the Upper Paleolithic and the newly agricultural Neolithic. The Epipaleolithic is divided into three major subdivisions: Kebaran (22,500–17,500 cal yr B.P.); Geometric Kebaran (17,500–14,900 cal yr B.P.); and Natufian (14,900–12,500 cal yr B.P.). The ages of these subdivisions are based on calibrated radiocarbon chronologies of others (e.g., Bar-Yosef, 1981, 1996; Goring-Morris, 1995; Goring-Morris and Belfer-Cohen, 1998).

The Kebaran complex was named by Garrod (1954) after the layers excavated by Turvill-Petre at Kebara Cave in the early 1930s (Turvill-Petre, 1932). The only thorough analysis of the Kebaran complex was in the 1960s (Bar-Yosef, 1970) and was later published in detailed overviews (Bar-Yosef, 1975, 1981). Bar-Yosef's study of Kebaran assemblages from the coastal plain, the mountainous areas in northern Israel, and the Jordan valley yielded not only a detailed definition of Kebaran lithic

Geoarchaeology: An International Journal, Vol. 18, No. 4, 461–475 (2003)

Published online in Wiley Interscience (www.interscience.wiley.com). DOI:10.1002/gea.10073

characteristics but also a subdivision of the Kebaran into four lithic facies/assemblages. The Kebaran is the earliest archaeological entity of the Epipaleolithic period and is spread over the Mediterranean zones of Israel. Kebaran sites have also been recorded in Lebanon, Syria, and Jordan (e.g., Byrd, 1998; Garrard et al., 1988; Muheisen, 1988). The Kebaran period is considered to have been a cold and dry phase at the end of the Pleistocene (Bar-Yosef, 1996; Goring-Morris and Belfer-Cohen, 1998). Kebaran sites are usually small in area, although larger open-air sites were explored in Jordan (e.g., Muheisen, 1988; Garrard et al., 1988).

Architectural features are rare at Kebaran sites and have been reported from the site of Ein Gev I (Arensburg and Bar-Yosef, 1973). The site of Ohalo II on the recently exposed floor of Lake Tiberias and dated to around 23,000 cal yr B.P. has rounded huts (e.g., Nadel and Werker, 1999), but it seems that this site is earlier than the Kebaran complex (e.g., Goring-Morris, 1995).

Kebaran finds, apart from rich flint assemblages, include ground stone tools (mostly mortars and pestles) as well as faunal remains. The economy has been reconstructed in very general terms and described as based on hunting and gathering, but details are few. The dominance of mountain gazelle *(Gazella gazella)* and fallow deer *(Dama mesopotamica)* among the game animals is clear (e.g., Davis, 1982; Bar-Oz and Dayan, 2002a); however, many other species also appear in Kebaran faunal collections (e.g., Saxon et al., 1978; Bar-Oz et al., 1999).

Research of the Kebaran complex in the Mediterranean zones of Israel has been sporadic in general and very sparse in the last two decades. At the same time, research on Epipaleolithic entities is advancing, mainly due to the work of Goring-Morris (1987, 1995) in the desert regions of Israel as well as in Jordan (e.g., Clark et al., 1988; Henry, 1989, 1995; Byrd 1998). However "normative" Kebaran was not defined in the desert of Israel and Jordan, and paralleling entities such as the Qalkhan (contemporaneous with the early Kebaran) and the Nizzanean (late Kebaran) were introduced (cf. Goring-Morris, 1995). The renewal of excavations at Hayonim cave and the work at the adjacent Kebaran rockshelter of Meged touch upon the Kebaran in the Mediterranean zones after a long gap in research (e.g., Barzilai, 2001).

Almost all of the Kebaran assemblages from the coastal plain are surface collections (Bar-Yosef, 1970) while *in situ* stratified sequences have been very limited. Kebaran coastal plain sites, when excavated, provide only very small exposed surfaces, usually not exceeding a few square meters and sometimes only single meters excavated as test pits (e.g., Saxon et al., 1978). Nahal Hadera V is exceptional in this regard being a site with a deep Kebaran stratigraphy (over 1 m) and recently re-excavated on a large scale exposing some 70 m^2 (Barkai and Gopher, 2001).

Kebaran sites, including Nahal Hadera V (NHV), contain plentiful faunal remains, and one would ordinarily expect ^{14}C dating to be the dating method of choice. Unfortunately, the high temperature and humidity of the region's climate, coupled with the very porous nature of coastal open-air sediments, result in such high rates of chemical weathering that bone collagen is too degraded for ^{14}C dating. Only a few Kebaran sites have ^{14}C ages associated with them (e.g., Bar-Yosef and Vogel, 1987; Byrd, 1998; Barzilai, 2001). Faunal material from NHV, submitted to the Weizmann Institute of Science Radiocarbon Laboratory, did not contain sufficient collagen for ^{14}C dating (E. Boaretto, personal communication, 2001). Thus, there is a clear need for alternative means of numerical dating to be applied to Epipaleolithic archaeological deposits of the Levant.

SITE DESCRIPTION

Nahal Hadera V is an open air site located on the coastal plain just northwest of the city of Hadera, Israel (map ref. 140.39-43/207.83-87), about 200 m south of the Hadera stream, and approximately 1 km east of the current shoreline of the Mediterranean Sea (Figure 1). Archaeological deposits at NHV are in a sand dune lying directly on a kurkar unit (carbonate-cemented aeolian sand). The site is located on a small hilltop and slopes downwards in all directions (Figure 2). The ancient landscape was probably flatter than it is today. The site appears to have been affected by deflation (on the hilltop) and erosion (mostly on the slopes). Occupation debris and lithic and faunal finds can be seen eroding on the hill slopes. The lithic assemblage is rich in microblade technology, small cores and microliths, and plentiful though fractured mammalian bone fragments (Bar-Oz and Dayan, 2002a, 2002b).

Nahal Hadera V contains an artifact assemblage attributed to the Kebaran cultural complex (Saxon et al., 1978; Barkai and Gopher, 2001). By Epipaleolithic standards, NHV is a large and intensively occupied site. The estimated area of the site is at least 500 m^2, and the thickness of its deposits is more than 1 m. Test excavation in the early 1970s revealed a sequence of six stratigraphic units of which at least two were characterized as occupation levels (Saxon et al., 1978).

During the 1997–1999 field seasons, a total of 70 m^2 were excavated in the central (highest) part of the site near the test excavation of the 1970s, and seven probes were placed in a lower part of the site to the south. A hutlike feature was revealed in the latest phase of the Kebaran sequence, as well as four to five superposed living floors to the south of it, indicating recurring occupation. Numerous flint and bone items were recovered using 0.25 m^2 excavation units, 5-cm-thick excavation levels, and screens (dry and wet) with 2.4 mm and 1 mm meshes. Groundstone tools and concentrations of flint and bone indicated activity areas. Lithic and bone assemblages were obtained from all occupational phases, including the lowermost and uppermost levels.

CRITERIA FOR OPTICAL DATING

In order for optical dating (Huntley et al., 1985) to be successful at a given site, several criteria must be met. First, the sediments of interest must contain sufficient quantities of the mineral chosen for analysis. Typically this is either quartz or feldspar, although other minerals such as calcite or zircon have been studied. Second, the mineral grains must have been exposed to the equivalent of at least several hours of full spectrum sunlight during deposition (Godfrey-Smith et al., 1988), after which they should have been completely buried and have remained in total dark-

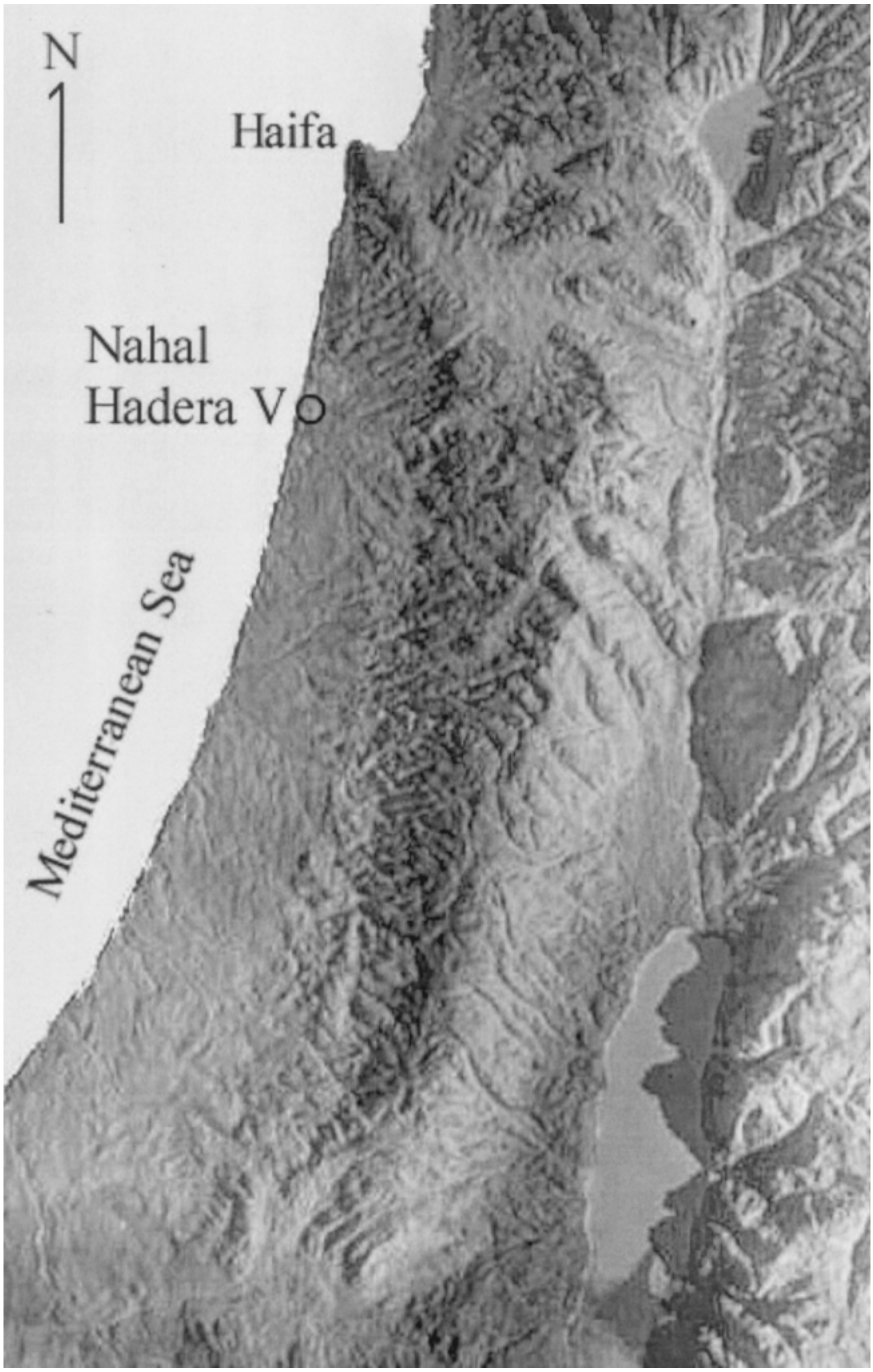

Figure 1. Location of Nahal Hadera V along the eastern Mediterranean coastline, shaded relief. Extending southeast from Haifa is the Carmel mountain range.

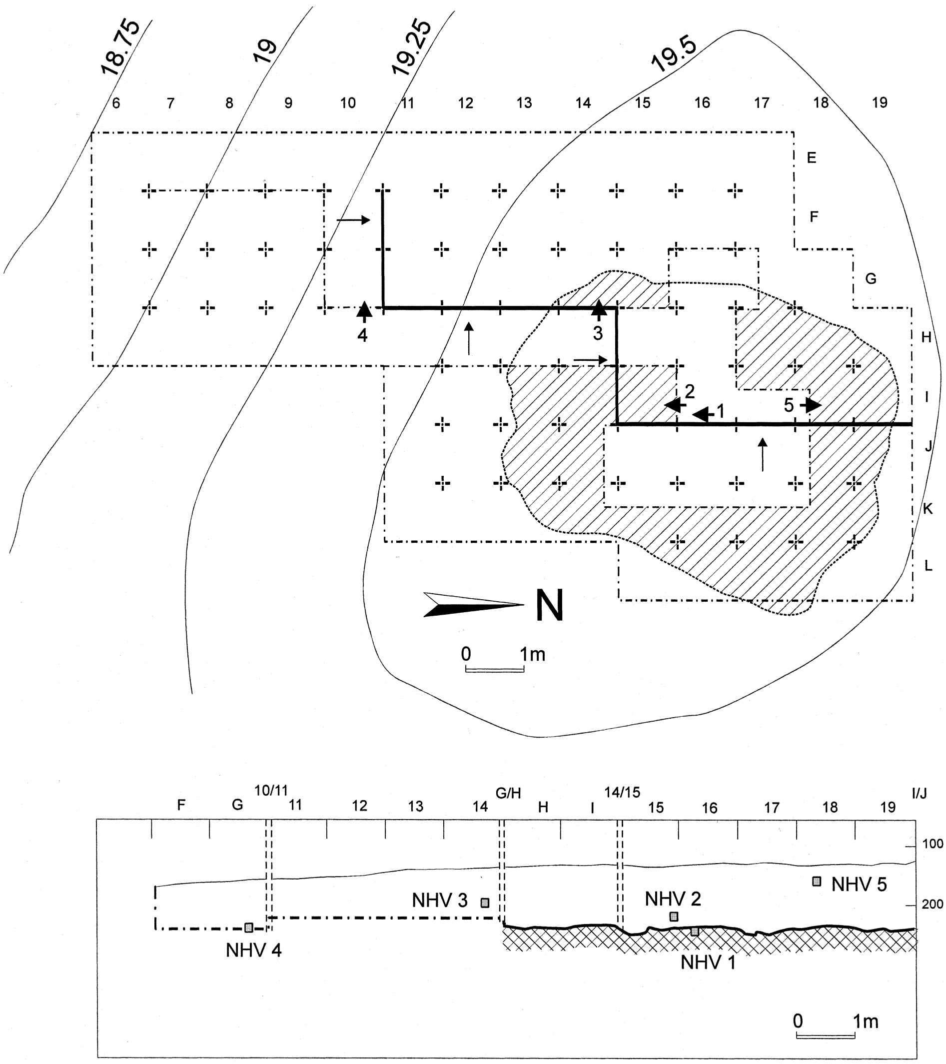

Figure 2. Plan (top) and section, showing locations of optical dating samples. Dash-dotted line (—·—) marks the boundaries of excavation. Hatched area in plan marks the extent of a dark brown soil with concentrated flint and bone. Contour lines are in meters above sea level. Stepped solid line and thin arrows in plan refer to the profile along which samples are shown. The heavy numbered arrows in plan correspond to sample numbers shown in profile. Vertical double dashed lines in the profile mark the turns. Hatched base in the profile indicates excavation to kurkar.

ness until sampling. Finally, the last exposure to light, which is the event being optically dated, should have taken place within the time range appropriate for the dating method. Depending on the concentration of the common radioisotopes in the sample, its burial depth, average moisture content, and the selected mineral's saturation response to large radiation doses, this is usually no more than a few hundred thousand years ago.

For this study, we chose to work with the quartz grains. Previous studies (Godfrey-Smith et al., 1988, Godfrey-Smith, 1991, 1994) demonstrated that quartz has an extremely favorable response to bleaching by natural sunlight. In addition, the extreme degree of insolation in the region means that the clock-resetting criterion necessary for optimal dating results is fulfilled. A recent study (Godfrey-Smith and Shalev, 2002) verified that sediments of the coastal plain of the eastern Mediterranean are rich in quartz mineral grains, and that these have favorable luminescence properties, which include an excellent dose response sensitivity, making them well suited to a chronological application. Although the upper limits for the optical dating of quartz are typically lower than the limits for feldspar, the postulated <40,000 year-age of the site all but guaranteed a successful outcome.

Nomenclatures in Radiocarbon and Luminescence Dating

In the previous discussion, we used calibrated years B.P. for dendrochronologically calibrated radiocarbon ages. By definition, this terminology is restricted to radiocarbon dates, and we deliberately avoid using it for luminescence dates (and, indeed, for numerical ages obtained by any other method). In luminescence dating, the notation ka is typically used for numerical ages equal to or greater than 1000 years (1 ka = 1000 years). We have chosen to retain this convention in our presentation of luminescence ages. The validity of this approach is made obvious when one considers that luminescence ages of, say, 65 ka are common in the literature, but an age of 65,000 cal yr B.P. cannot occur because of the limitations of both the radiocarbon dating method and existing calibration curves. In spite of the deliberate notational differences, a luminescence age of 20 ka and a radiocarbon age of 20,000 cal yr B.P. both refer to the secular time scale and are equivalent to 20,000 calendar years ago.

SAMPLE DESCRIPTIONS

The samples collected for optical dating are mapped in Figure 2 with respect to the 1997-1999 excavation.

NHV1. Unit I16D, 221 cm b.d. (below datum). Kurkar aeolianite fragment, 12 × 17 × 5 cm, immediately below contact with overlying soft sediments. The natural surface of the site at sample locations 1 and 2 is 120 cm below datum. Because the sample was in contact with overlying sediments that were different than the kurkar, separate dosimetry samples for gamma dose rate measurements were also collected. These are NHV-1A (subkurkar) and NHV-1B (superkurkar, 0–3 cm above the upper surface of the kurkar, in overlying brown sediment).

NHV2. Unit I15B, 210 cm b.d., soft brown sediment from the north wall of unit I15, 13 cm from its east wall, and 11 cm above its contact with the kurkar. This is a subcultural phase located below the earliest occupation of the site and above the kurkar.

NHV3. Unit G14B, 190 cm b.d., sampled from its east wall. Living floor plus sub-living floor sediments. Since the living floor is 175–185 cm b.d., and the sediment sample was centered at 190 cm, one half to a third of the sediment collected is in the subunit below the living floor.

NHV4. Unit G10B, 238 cm b.d., sampled from the unit's east wall. The living floor here is at 205–212 cm b.d. The kurkar's upper surface is not exposed at this location, although it is found at a much lower elevation.

NHV5. Unit J18C, 164 cm b.d., sampled from south to north, 21 cm east of boundary with unit I, about 30 cm below surface. This sample constitutes the fill of a housepit feature, a very dense concentration of flint artifacts and bone fragments in dark brown to black sediment.

METHODS

Sample Preparation and Analysis

The bulk sediment was treated with HCl and H_2O_2 to remove carbonates and organics, and dry sieved to obtain fine sand size grains in the narrow range of 90–125 μm. Most nonquartz minerals were removed using two heavy liquid separations which removed grains with densities <2.60 and >2.70 g cm^{-3}, and magnetic separation. The remaining quartz-dominated grains were treated with concentrated HF, which dissolved the remaining nonquartz minerals and removed the outer 20 μm layer of the quartz grains themselves. The purified quartz extract was re-sieved through a 90 μm screen to remove fragments of grains broken during treatment.

Dosimetry

Potassium concentrations were determined by x-ray fluorescence at the Geochemistry Centre, St. Mary's University, Halifax. A 5% error in the measured K_2O value is included in the dose rate calculation. Uranium (U) and thorium (Th) concentrations were measured using thick-source alpha counting of samples crushed to a fine powder, which had rested for >1 month after crushing before being measured (Table I). The great advantage of alpha counting over more precise determinations of U and Th (for example, INAA and DNA) is that it determines the true activity of each radioisotope chain in its entirety, and thus naturally compensates for any disequilibria which may be present in the sediment. Thus, although the equivalent U and Th concentrations (Table II) are not of high precision, the actual dose rate variation due to all dosimetry variables, excluding moisture content, is <3%. Inclusion of the moisture content error increases the error in the dose rate to <6%. No moisture content measurements were done; instead, an assumed value of 0.06 ± 0.05 (6% water, as a percentage of dry sediment weight) was used, which reflects both Holocene seasonal winter/summer variations and a probable higher

Table I. Dosimetry values for Nahal Hadera V.[a]

Nahal Hadera V Sample	Depth m b.d.[b]	Depth m b.s.[b]	Moisture Content	Bulk K_2O%	Alpha counts (ks^{-1} cm^{-2}) Total	Th
NHV 1: kurkar cemented dune	2.25	1.05	0.06	0.32	0.105±0.005	0.018±0.009
NHV 2: immediately above kurkar	2.10	0.80	0.06	0.62	0.263±0.007	0.106±0.022
NHV 3: living floor + sub-floor	1.90	0.50	0.06	0.64	0.313±0.008	0.092±0.021
NHV 4: immediately below living floor	2.38	0.60	0.06	0.62	0.314±0.008	0.103±0.022
NHV 5: housepit feature	1.64	0.34	0.06	0.52	0.283±0.008	0.098±0.022

[a]Average grain size = 115 μm. Standard errors assumed for moisture content and K_2O, are 0.05 and 5% of measured value, respectively.
[b]b.d. = below datum, b.s. = below surface.

moisture content during the late Quaternary. The coarse, highly porous, and well-drained nature of the sediments makes it unlikely that average yearly moisture contents could have fluctuated outside the moisture content's assumed error (±0.05).

D_e Determinations

Single aliquot additive dose (SAA) analysis was used to determine the past D_e (Duller, 1994). For each sample, 15 aliquots were prepared by depositing 10–15 mg of quartz extract in a monolayer on 0.98 cm Al disks. All aliquots were preheated at 230°C for 300 s and stimulated with a narrow band of green photons for 0.5 s. Detection was through a stack of ultraviolet-transmitting Schott U340 glass filters. In order to prevent charge re-trapping in the 100°C TL trap and avoid second-order effects, all optical stimulations were performed at 120°C.

During each additive dose analysis, an aliquot was given six irradiations in the range of 10–150 Gy. For sample NHV5, the initial set of measurements yielded a significantly lower D_e than expected; thus a second set of 10 aliquots was analyzed,

Table II. Alpha-equivalent U and Th concentrations.[a]

Nahal Hadera V (Sample)	U (ppm)	Th (ppm)
NHV 1: kurkar cemented dune	0.68±0.35	0.48±0.24
NHV 2: immediately above kurkar	1.23±0.55	2.85±0.59
NHV 3: living floor + subfloor	1.73±0.63	2.47±0.56
NHV 4: immediately below living floor	1.65±0.63	2.77±0.59
NHV 5: housepit feature	1.45±0.63	2.63±0.59

[a]Based on the following conversion factors: Th ppm = Th counts/0.0372; U ppm = Total − Th counts/0.128.

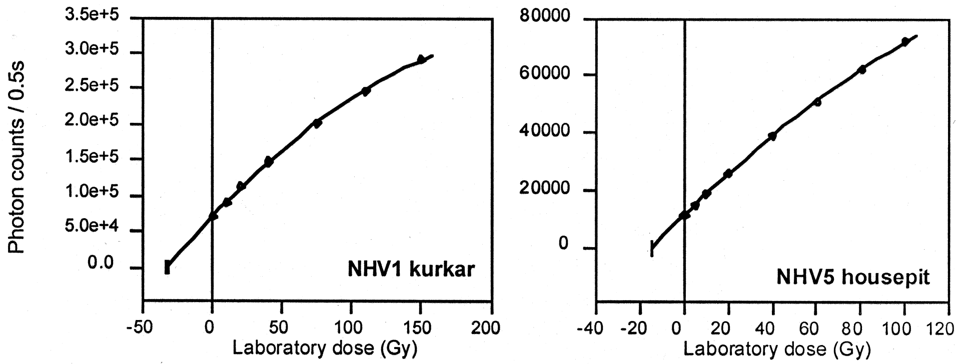

Figure 3. Growth curves for NHV1 and NHV5. The past dose D_e is centered between the two short vertical dashes (not resolvable at this scale) which define ±1 standard deviation, at lower left of the extrapolated curve. The $x = 0$ axis is omitted for clarity.

with added doses of 10–100 Gy only. The average D_e's obtained in the two runs were statistically identical.

A preheat calibration was performed on each aliquot independently of all other aliquots, after the aliquot's additive dose run, with eight preheat + shine cycles identical to those used in the additive dose run. This procedure was tested on a quartz extract from an African sediment that was completely bleached with natural light and re-irradiated with 4.4 Gy. It yielded a mean $D_e = 4.46 \pm 0.30$ Gy ($\sigma_M = \pm 0.09$ Gy, n = 10). The validity of the SAA method for dating quartz-rich sediments within the Epipaleolithic time frame was verified in an earlier study (Ivester et al., 2001). A past D_e was obtained for each aliquot by extrapolation of a least squares fit of the preheat-corrected dose response growth curve, with inverse weighting with respect to intensity. The additive dose growth curves were only slightly sublinear; quadratic fits were made to the data using a published least squares routine (Noggle, 1993). Typical growth curves and D_e extrapolations for NHV1 and NHV5 demonstrate the maximum and minimum degrees of sublinearity shown by quartz of this site and are presented in Figure 3.

DISCUSSION OF LUMINESCENCE AGES

As expected, the sediments at NHV contain plentiful quartz sand. Because of the high geological maturity of the sediments, the relative proportion of feldspar minerals is extremely low. This is reflected by the very low potassium contents. Uranium and thorium concentrations in the archaeological sediments (U 1.2–1.7 ppm, Th 2.5–2.9 ppm) are about one third of typical concentrations of most clastic sediments, and they are very low (U 0.7, Th 0.5 ppm) in the carbonate-rich kurkar. Cosmic dose rates were estimated on the basis of present depths below surface and ranged from 0.18 to 0.2 Gy/ka. Beta dose rates were calculated based on each sample's own values; however, the gamma dose rates (R_γ) were adjusted for the <30 cm proximity of non-self sediments in two cases. For NHV2, the gamma dose rate was based on 0.9 self R_γ plus 0.1 NHV1 R_γ.

The case for NHV1, the kurkar sediment, was somewhat more complex, because we had to make some reasonable assumptions regarding the sample's past geomorphic history. Based on the 21.3 ka age we obtained for the overlying NHV2 (see below) and the ages for NHV3–NHV5, which indicated that the overlying archaeological sediments were deposited rapidly, we based the gamma dose rate for the time period 21.3 ka–present, on 0.7 self R_γ plus 0.3 R_γ of the adjacent NHV2, for an overall dose rate R = 0.68 Gy/ka. Before 21.3 ka, however, the overlying sediment (NHV2) did not exist, thus the gamma dose rate for the pre-21.3 ka time range is 100% self R_γ, and R = 0.61 Gy/ka.

The sediment of NHV5 was exceptionally rich in flint flakes. Based on estimates of total flint debitage recoveries from the adjacent 0.5 × 0.5 m subunits, the composition of this unit is 10% flint by weight. Because flint is radioisotope-depleted in comparison to the sediment matrix, it acts as an inert diluant for the γ dose rate. Because the flakes collected with the matrix during sampling were deliberately excluded from crushing for alpha counting, the γ dose rate for NHV5 was reduced to 0.9 self R_γ to correct for radioisotope dilution by the flint.

Mean past doses, dose rates, and ages are shown in Table III. Ages for the archaeological sediments ranged from 21.3 ± 2.3 to 18.3 ± 2.2 ka for the main deposit, and 14.0 ± 2.1 ka for intrusive sediments in the Kebaran housepit feature. The ages of greatest interest are NHV3 and NHV4. NHV3 was taken directly below an artifact (flint) and bone-rich layer (locus 175) at 175–185 cm b.d. NHV4 was taken below another artifact and bone-rich living floor to the south (locus 100) at 202–215 cm b.d. Thus, the lower living floor (locus 100) is securely dated between 21.3 ± 2.3 and 18.3 ± 2.2 ka. Locus 175, the upper living floor, postdates 18.3 ka but is defi-

Table III. Past doses, dose rates, and ages for Nahal Hadera V.[a,b]

Nahal Hadera V Sample	Past dose D_e (Gy)	Dose rate R (Gy/ka)	Age (ka)
NHV 1: kurkar cemented dune	27.40±2.25	**0.68[a]±0.09** **0.61[b]**	42.7±6.3[c]
NHV 2: immediately above kurkar	23.65±2.20	**1.11±0.07**	21.3±2.3[c]
NHV 3: living floor + subfloor	22.76±2.46	**1.24±0.07**	18.3±2.2[c]
NHV 4: immediately below living floor	24.97±2.95	**1.23±0.07**	20.3±2.7[c]
NHV 5: housepit feature	14.00±1.95	**1.00±0.06**	14.0±2.1[c]

[a]Dose rate for 21.3 ka–present.
[b]Dose rate since kurkar formation until 21.3 ka ago, for depth = 1.05 m.b.s. See text for details.
[c]The uncertainty in the age is calculated by adding in quadrature the standard deviation σ in past dose D_e and the combined measured errors in dose rate R, both given here. We note, however, that it has become commonplace since the introduction of the SC-SAR single aliquot regeneration method of luminescence dating (Murray and Wintle, 2000) to use the *standard error of the mean* σ_M in age calculations, where $\sigma_M = \sigma\, n^{-1/2}$, and n = number of independent D_e determinations. In our data, n = 12 for samples NHV1 and NHV2, and 14 for the remaining samples. Use of σ_M reduces the errors associated with the quoted ages to: 5.5, 1.4, 1.2, 1.3, and 1.0 ka, for samples NHV1 to NHV5, respectively.

nitely earlier than the fill of the house pit feature (sample NHV5) dated at 14.0 ± 2.1 ka. Ongoing analyses of more tightly defined (in a vertical sense) samples of the upper living floor and horizons immediately above it are expected to resolve the ages with more precision.

Results of the single aliquot D_e determinations are shown in Figure 4. Some variation in the D_e's is observed. This is an expected consequence of variations in natural sedimentation rates. Based on the depths below the living floor of NHV3 and NHV4, and the 2 ka difference in their ages, we estimate an average depositional rate at the site of 10 cm/ka. Therefore, a finite, 6-cm-thick vertical slice (the thickness of the sampling container) of the archaeological sediments should contain a mixture of quartz grains that were last exposed to light at least 600 years apart. Additional disturbance due to faunal and floral bioturbation would be expected to widen this range by transporting older grains from lower horizons upward and younger grains downwards.

The geological substrate underlying the archaeological deposit is a quartz-rich, carbonate-cemented aeolianite or kurkar. Its luminescence age is 42.7 ± 6.3 ka. We emphasize that, in the absence of empirical evidence, the modern depth below surface (1.05 m) was used in the dose rate calculation, a variable which relates to the cosmic dose rate via the equation

$$c = 0.21 \exp(-0.07 \times 2d + 0.0005 \times 4d^2),$$

where c = cosmic dose rate and d = depth below surface in meters (Prescott and Hutton, 1988).

Though this depth is likely to be correct, on average, for the post-21.3 ka period, we do not know how closely it approximates the average depth prior to that time. Because the kurkar is a friable material unlikely to sustain a stable geomorphic surface for >20 ka, we believe that an average depth <1 m is unlikely. It is possible, however, that the kurkar aggraded rapidly to a much greater height and eroded quickly during the last glacial maximum. Thus, at 1.05 m average depth, c is 0.182 Gy/ka. However, if the average depth was 5 m, c would be reduced to 0.110 Gy/ka, and the kurkar's age would increase to 45.6 ka; if the pre-21.3 ka average depth was 10 m, the age would increase to 48 ka. Because of the uncertainties in the kurkar's ancient depth below surface and the resulting potential for age differences, it is best to accept 42.7 ka as a minimum age for the kurkar. We stress that such large depth-related age changes are atypical in most clastic-rich sediments, in which self dose rates are >2 Gy/ka and the cosmic dose rate is, therefore, a much smaller fraction of the total R. The depth variations are significant to the age estimate of NHV1 because radioisotope-poor carbonates and quartz dominate this sediment, and therefore its self β and γ dose rates are very low. They would be equally significant in other quartz-dominated, very mature sediments (Ivester et al., 2001). In any event, we suggest that the kurkar is cognate with the Dor Kurkar exposed at the Givat Olga section, which has yielded an average age of 54 ± 9 ka based on IRSL dating of potassium feldspar grains (Frechen et al., 2002). Individual IRSL

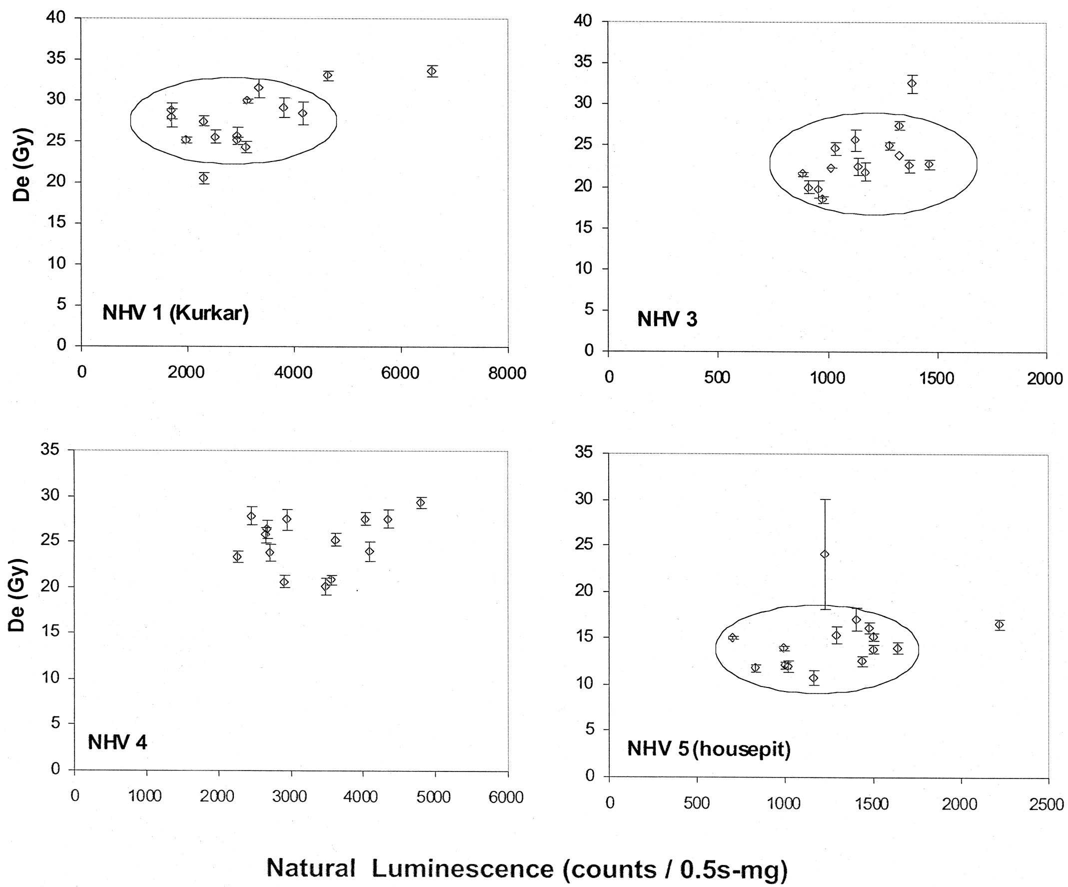

Figure 4. Scattergrams of single aliquot D_e versus that aliquot's natural luminescence per unit mass. Samples included in the calculation of mean D_e are inside the ellipses. No ellipse is drawn around the data in NH4, because all points were included in the mean D_e.

ages for this kurkar at the Givat Olga and the Netanya South sections range from 32 to >80 ka (Frechen et al., 2002).

CONCLUSION

We have obtained the first direct luminescence ages for a Kebaran period archaeological site, Nahal Hadera V. These ages suggest that human occupation of the site occurred between 21.3 and 14.0 ka. This time range places the site's occupation within marine oxygen isotope stage 2, the Last Glacial Maximum (Martinson et al., 1987). During this stage, sea levels worldwide were 60–120 m lower than they are today because of the mass of oceanic water bound within continental ice sheets. Hence, the coastline of the Mediterranean Sea, now within 1 km of the site, would have been several kilometers further west.

The direct luminescence dates for NHV bracket specific living floors between 20.3 and 18.3 ka and can be compared with ^{14}C ages for other Kebaran sites. The available Kebaran ^{14}C ages include series or single determinations made in the last three decades from several sites in Israel and Jordan. These include Rakefet Cave, Nahal Oren, Ein-Gev (Arensburg and Bar-Yosef, 1973), Kharaneh (Muheisen, 1988), Wadi el-Jilat 6 (Garrard and Byrd, 1992), and Meged rockshelter (Barzilai, 2001). Additional ^{14}C ages from Jordan are reported in Byrd (1998:67–69) and include dates from the following Kabaran sites: Uwaynid 14 and 18; Wadi Hammeh 26, 31, 50, 51, and 52; Tor el Tareeq; and Madamagh and Tabaqat el-Buma. When calibrated, these ages range from 21,700 cal yr B.P. (not including one earlier date from Meged rockshelter) to 16,800 cal yr B.P. The NHV dates we have obtained thus far are in accordance with the middle to late part of this range. The results of the lithic analysis of NHV assemblages support this conclusion.

Direct luminescence dating of sand has great potential for developing a numerical chronology for coastal plain Epipaleolithic sites in the Levant and should become a routine procedure.

Financial support for this study was provided by the Natural Sciences and Engineering Research Council (NSERC) of Canada, through a discovery grant to D.I. Godfrey-Smith. Topographic information shown in Figure 2 was obtained during the 1997–1999 excavation, which was supported by the Israel Science Foundation (Grant 794/98), the Irene Levi Sala CARE Archaeological Foundation, and MAFCAF Foundation.

REFERENCES

Arensburg, B., & Bar-Yosef, O. (1973). Human remains from Ein Gev I, Jordan Valley, Israel. Paléorient, 1/2, 201–206.

Barkai, R., & Gopher, A. (2001). Nahal Hadera V. Hadashot Arkheologiyot. Excavations and Surveys in Israel, 113, 35.

Bar-Oz, G., Dayan, T., & Kaufman, D. (1999). The Epipalaeolithic faunal sequence in Israel: A view from Neve David. Journal of Archaeological Science, 26, 67–82.

Bar-Oz, G., & Dayan, T. (2002a). "After 20 years": A taphonomic reevaluation of Nahal Hadera V, an Epipalaeolithic site on the Israeli coastal plain. Journal of Archaeological Science, 29, 145–156.

Bar-Oz, G., & Dayan, T. (2002b). Taphonomic analysis of the faunal remains from Nahal Hadera V. In

H. Buitenhuis, A.H. Al-Shiyab, M. Mashkour, & A. Choyke (Eds.), Archaeozoology of the Near East V (pp. 40–47). Groningen: Groningen Institute for Archaeology.

Bar-Oz, G., Dayan, T., & Kaufman, D. (1999). The Epipalaeolithic faunal sequence in Israel: A view from Neve David. Journal of Archaeological Science, 26, 67–82.

Bar-Yosef, O. (1970). The Epi-Paleolithic cultures of Palestine. Unpublished doctoral dissertation, The Hebrew University, Jerusalem.

Bar-Yosef, O. (1975). The Epi-Paleolithic in Palestine and Sinai. In F. Wendorf & A.E. Marks (Eds.), Problems in prehistory: North Africa and the Levant (pp. 363–378). Dallas, TX: Southern Methodist University Press.

Bar-Yosef, O. (1981). The Epi-Paleolithic complexes in the southern Levant. In J. Cauvin & P. Sanlaville (Eds.), Prehistoire du Levant: Chronology et l'organisation de l'espace depuis les Origines jusqu'au Vie Millenaire (pp. 389–408), Colloque Internationaux du C.N.R.S. No. 598. Lyon, France: Maison de l'Orient.

Bar-Yosef, O. (1996). The impact of late Pleistocene-early Holocene climatic changes on humans in Southwest Asia. In L.G. Straus, B. Eriksen, J.M. Erlandson, & D.R. Yesner (Eds.), Humans at the end of the Ice Age. The archaeology of the Pleistocene–Holocene transition (pp. 61–78). New York: Plenum Press.

Bar-Yosef, O., & Vogel, J.C. (1987). Relative and absolute chronology of the Epi-Paleolithic in the Southern Levant. In O. Aurenche, J. Evin, & F. Hours (Eds.), Chronologie du Proche-Orient, 16.000–4.000 B.P.(pp. 219–245). Oxford: British Archaeological Reports.

Barzilai, O. (2001). The lithic assemblage of Meged Rockshelter (1995–1997 excavations). Unpublished master's thesis, The Hebrew University, Jerusalem.

Byrd, B. (1998). Spanning the gap from the Upper Paleolithic to the Natufian: the Early and Middle EpiPaleolithic. In D.O. Henry (Ed.), The prehistoric archaeology of Jordan (pp. 64–82), BAR International Series 705. Oxford: British Archaeological Reports.

Clark, G., Lindly, J., Donaldson, M., Garrard, A.N., Coinman, N., Schuldenrein, J., Fish, S., & Oleszewski, D. (1988). Excavations at Middle, Upper and EpiPaleolithic sites in the Wadi hasa, West Central Jordan. In A.H. Garrard & H.-G. Gebel (Eds.), The prehistory of Jordan (pp. 209–285), BAR International Series 396. Oxford: British Archaeological Reports.

Davis, S.J.M. (1982). Climate change and the advent of domestication: The succession of ruminant artiodactyls in the late Pleistocene-Holocene in the Israel region. Paléorient, 8, 5–15.

Duller, G.A.T. (1994). Luminescence dating using single aliquots: New procedures. Quaternary Geochronology (QSR) 13, 149–156.

Frechen, M., Neber, A., Dermann, B., Tsatskin, A., Boenigk, W., & Ronen, A. (2002). Chronostratigraphy of aeolianites from the Sharon Coastal Plain of Israel. Quaternary International 89, 31–44.

Garrard, A.N., & Byrd, B.F. (1992). New dimensions to the Epipalaeolithic of the Wadi el-Jilat in central Jordan. Paléorient, 18, 47–62.

Garrard, A.N., Betts, A., Byrd, B., & Hunt, C. (1988). Summary of paleoenvironmental and prehistoric investigations in the Azraq Basin. In A.H. Garrard & H.-G. Gebel (Eds.), The Prehistory of Jordan (pp. 311–337), BAR International Series 396. Oxford: British Archaeological Reports.

Garrod, D. (1954). Excavations at the Mugharet Kebara, Mount Carmel, 1931. Proceedings of the Prehistoric Society, 20, 155–192.

Godfrey-Smith, D.I. (1991). Optical dating studies of sediment extracts. Unpublished doctoral dissertation, Simon Fraser University, Burnaby, Canada.

Godfrey-Smith, D.I. (1994). Thermal effects in the optically stimulated luminescence of quartz and mixed feldspars from sediments. Journal of Physics D: Applied Physics, 27, 1737–1746.

Godfrey-Smith, D.I., & Shalev, S. (2002). Determination of usage and absolute chronology of a pit feature at the Ashkelon Marina, Israel Early Bronze I archaeological site. Geochronometria, 21, 163–166.

Godfrey-Smith, D.I., Huntley, D.J., & Chen, W.-H. (1988). The optical behaviour of quartz and feldspar sediment extracts. Quaternary Science Reviews, 7, 373–380.

Goring-Morris, A.N. (1987). At the edge. Terminal Pleistocene hunter-gatherers in the Negev and Sinai, BAR International Series 361. Oxford: British Archaeological Reports.

Goring-Morris, N. (1995). Complex hunter-gatherers at the end of the Paleolithic. In T.E. Levy (Ed.), Archaeology of society in the Holy Land (pp. 141–168). London: Leicester University Press.
Goring-Morris, N., & Belfer-Cohen, A. (1998). The articulation of cultural processes and Late Quaternary environmental changes in CisJordan. Paléorient, 23, 71–93.
Henry, D.O. (1989). From foraging to agriculture: The Levant at the end of the Ice Age. Philadelphia: University of Pennsylvania Press.
Henry, D.O. (1995). Prehistoric cultural ecology and evolution: Insights from southern Jordan. New York: Plenum Press.
Huntley, D.J., Godfrey-Smith, D.I., & Thewalt, M.L.W. (1985). The optical dating of sediments. Nature, 313, 105–107.
Ivester, A.H., Godfrey-Smith, D.I., & Leigh, D.S. (2001). Chronology of source-bordering dunes in the Coastal Plain of Georgia, U.S.A. Quaternary Research, 55, 293–302.
Martinson, D.G., Pisias, N.G., Hays, H.D., Imbrie, J., Moore, T.C., & Shackleton, N.J. (1987). Age dating and the orbital theory of the Ice Ages: Development of a high-resolution 0 to 300,000 year chronostratigraphy. Quaternary Research, 27, 1–29.
Muheisen, M. (1988). The Epipalaeolithic phases of Kharaneh IV. In A.H. Garrard & H.-G. Gebel (Eds.), The prehistory of Jordan (pp. 353–367), BAR International Series 396. Oxford: British Archaeological Reports.
Murray, A.S., & Wintle, A.G. (2000). Luminescence dating of quartz using an improved single-aliquot regenerative-dose protocol. Radiation Measurements, 32, 57–73.
Nadel, D., & Werker, E. (1999). The oldest ever brush hut plant remains from Ohalo II, Jordan Valley, Israel (19 ka BP). Antiquity, 73, 755–764.
Noggle, J.H. (1993). Practical curve fitting and data analysis. Englewood Cliffs, NJ: Prentice Hall.
Prescott, J.R., & Hutton, J.T. (1988). Cosmic ray and gamma ray dosimetry for TL and ESR. Nuclear Tracks and Radiation Measurements, 14, 223–227.
Saxon, E.C., Martin, G., & Bar-Yosef, O. (1978). Nahal Hadera: An open-air site on the Israeli littoral. Paléorient, 4, 253–266.
Turvill-Petre, F. (1932). Excavations at the Mugharet el-Kebara. Journal of the Royal Anthropological Institute, 62, 271–276.

Received September 5, 2002
Accepted for publication October 23, 2002